Chapter 26
Regional Rupture-Based Seismic Hazard Analysis of Tripura State—NE India

P. Anbazhagan, Arindam Das, and G. Silas Abraham

Introduction

The north-eastern state of India, Tripura, is located between two of the most tectonically active plate boundaries, the Indian-Sunda plate boundary in the east and the Indian-Eurasian plate boundary in the north. The Indian plate is moving under the Eurasian plate as well as the Sunda plate at the boundaries. In the past few decades, many destructive earthquakes were recorded in the region. The Shillong earthquake of 1897, Bihar-Nepal earthquake of 1934, and Assam earthquake of 1950 are some of the mass devastating earthquakes. Recently in 2017, a 5.6 magnitude earthquake at Manu induced liquefaction and also damaged more than 6000 houses in many parts of the state [5, 16]. The rapidly growing population resulting in industrialization and urbanization have intensified the hazard. Hence, currently used construction practices need an upgradation to account for the regional seismicity to mitigate the hazard of the region. The design PGA given in IS 1893 [25] is 0.36 g for the entire state of Tripura. However, the Indian standard code provides the zonation map considering only the past seismic activity of the region and does not consider other factors, like the rupture mechanism and the tectonic features of the area. Therefore, seismic hazard analysis for the region should be carried out in detail, considering all the seismotectonic features, rupture mechanisms, and past seismicity. This study provides the spatial distribution of the bedrock Peak Ground Acceleration for the state of Tripura by DSHA. The seismic hazard of the state was analysed using rupture-based approach (considering the rupture characteristic of the region) and the conventional approach (considering the observed magnitudes from the past seismic activities) both to understand better the influence of rupture characteristics in the seismic hazard analysis for the region.

P. Anbazhagan (✉) · A. Das · G. Silas Abraham
Department of Civil Engineering, Indian Institute of Science, Bangalore 560012, India
e-mail: anbazhagan@iisc.ac.in

K. Muthukkumaran et al. (eds.), *Soil Dynamics, Earthquake and Computational Geotechnical Engineering*, Lecture Notes in Civil Engineering 300,
https://doi.org/10.1007/978-981-19-6998-0_26

Study Area and Its Tectonic Framework: Tripura

Tripura, one of the hilly states of North-East India, is bordered on three sides by Bangladesh. The capital of Tripura is Agartala which is situated near the Bangladesh border in the north-western part of the state. The third-smallest state in the country, Tripura, has an area of 10,486 km^2. In 2011, the state had 36,71,032 residents, constituting 0.3 per cent of the country's population. There are few seismically active regions of the country, and Tripura is one of them. As per the IS 1893 part-1 (2016), the whole state of Tripura is in seismic zone V. The map of Tripura is presented in Fig. 26.1. The red coloured stars in the figure represent the earthquakes whose felt intensity was IV in Tripura and were considered for choosing the seismic study area.

Hills, plains, and valleys characterize the topography of Tripura. The geology of Tripura shows a variety of sedimentary rocks that dates back to the Oligocene period as per Tripura state pollution control board.

The whole North-East India has a high seismicity. The tectonic environment of the region is very complex. Thingbaijam et al. [42] pointed out that the seismic activities of the region include intraplate activities, subduction, and thrusting. Main Boundary Thrust (MBT), Dauki fault, Sagaing fault, Main Central Thrust (MCT), Main Frontal Thrust (MFT), etc., are some of the major active seismic sources in the region. In the past, these faults had significantly ruptured causing some of the major devastating earthquakes.

Various researchers have studied the regional seismotectonics and found: Indian and the Eurasian plates are converging in the north resulting in the formation of the

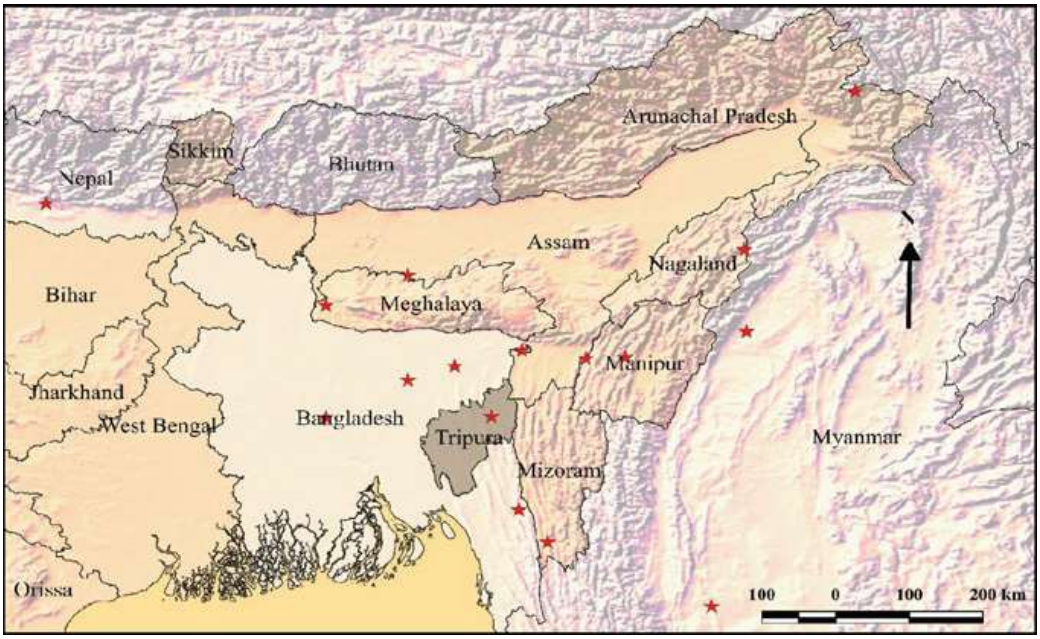

Fig. 26.1 Geographic location of Tripura

Himalayan range and due to subduction activity, in the east, of the Indian plate and the Sunda plate, the Indo-Burmese Ranges are created.

The tectonics of the study area include Himalayan thrust zone, Bengal basin and Shillong plateau, and the Indo-Burmese subduction zone which are in the northern side of the state, eastern side of the state, and western side of the state, respectively, as per Anbazhagan and Balakumar [5].

Himalayan Belt

The seismicity of the Himalayan belt trending from east to west is well explained by the converging of the Indian plate under the Eurasian plate, leading to the creation of the mountain arc of Himalayas. The Main Central Thrust (MCT), Main Frontal Thrust (MFT), and Main Boundary Thrust (MBT) are the major thrust faults in the Himalayan Arc [27]. These faults delineate the boundary of convergence between the two plates. The dipping of the Indian plate below the Eurasian plate is occurring at an approximate rate of 4.5 cm/year [11]. Moreover, Bilham [11] suggested the probable existence of many faults in the region waiting for potential reactivation. The range of Himalaya is not equally seismogenic, indicating the presence of non-uniform seismic slip. From the observations of paleoseismic, microseismic, and modern Global Positioning System, Srivastava et al. [39] located around ten seismic gaps in the Himalayan ranges. The seismic gaps are the Kashmir gap, Kangra gap, Jammu gap, Eastern Himachal Pradesh gap, Western Nepal gap, Sikkim Bhutan gap, Central Nepal-Bihar gap, Shillong gap, and Arunachal gap as mentioned by the above study. But among these gaps, the Shillong, Arunachal, and Sikkim Bhutan gap are the gaps of concern for this present study.

Indo-Burma Ranges (IBR)

The Indo-Burma ranges located in the eastern part of the study area (SA) is the intraplate boundary between the Indian and Burmese plates. The north-western part of the Sunda plate is formed by the Indo-Burma ranges and the Sagaing fault. The Indo-Burma ranges are almost trending from north to south and meet the Himalayan Arc at the Eastern Himalayan Syntaxis. A study by Kundu and Gahalaut [28] reported that in the Indo-Burma wedge, the focal mechanism involves strike-slip or thrust faults, while the Sagaing fault exhibits the focal mechanism of strike-slip. The Indo-Burma wedge shows much deeper earthquake events as compared to the Sagaing fault. Recently, Steckler et al. [40] studied the GPS data along the plate boundaries and reported that the Indo-Burma region is still having active subduction. They discovered the accumulation of convergence exceeding 5.5 m in the Indo-Burma wedge over the past 400 years, suggesting that an 8.2–9 M_W mega-thrust earthquake is likely to occur in that region in future. Wang et al. [44] divided this region into five major

regimes depending on tectonics and seismicity, namely the Indo-Burma subduction zone, Naga zone, Dhaka zone, Shan zone, and Sagaing zone. The empirical relations provided by different researches indicate that the seismic sources in this area have capacity to produce an earthquake with $M_W = 7$. However, incomplete rupture of the faults will result in earthquakes with smaller magnitude.

Shillong Plateau

Shillong plateau can be regarded as the projection of the Indian shield in the north-eastern direction which is surrounded by the Himalayan Arc, Dauki fault, and Assam Syntaxis in the north, south, and northeast, respectively. This plateau, which is also known as Shillong Mikir Massif, had risen to an elevation of about 1000 m in the geological past [27]. This region shows intraplate earthquakes such as the Shillong earthquake of 1897.

Bengal Basin

The Bengal basin, in the south of the Dauki fault, is one of the world's largest sedimentary basins which is created by the flowing rivers in that region. This basin possesses its own complex tectonic features, which can be categorized into four major zones, namely (i) Eocene Hinge Zone, the tectonic feature trending in NE-SW, (ii) north-western shelf zone, (iii) southeast deep basin, and (iv) western shear zone [30]. Most of the regions in this basin face the threat of seismic hazards. Due to interplate activities, the seismic activity in the fold belt of Tripura is higher than that in the Eocene Hinge Zone. The Bengal basin is characterized by thick sediment deposits and less crustal thickness. The sediment deposits can intensify the ground motion by 3–4 times, as they did during the Shillong earthquake, 1897. There is a high probability of liquefaction in that region due to the presence of wet sediments [41]. Rao et al. [33] investigated the cause of the magnitude M_W 6 earthquake that occurred in the Bay of Bengal, on May 21, 2014. The reason behind the earthquake might be the reactivation of a strike-slip fault zone of the Precambrian era in the lithosphere of the ocean.

Preparation of Seismotectonic Map

Seismotectonic map should be comprised of all the faults, lineaments, seismic gaps, and past seismic events of the seismic study area (SSA) which can affect the study area (SA). The seismotectonic map is essential to get an overall view of the seismic

status of the SSA and to forecast future seismic hazards of the SA [8]. The earthquake catalogue and all the seismic sources of the SSA are compiled, to prepare the seismotectonic map, from different sources.

Selection of Seismic Study Area (SSA)

As suggested by Anbazhagan et al. [6], the past damage intensity maps, i.e. isoseismal maps of the region, should be studied for selecting the SSA for any hazard analysis. The selection of SSA should be done in such a way that it captures all the past earthquake events and potential seismic sources that might cause damage to the study area. Generally, for damage to the structures and other facilities, intensity of IV or V on the Modified Mercalli Intensity (MMI) scale is considered to be sufficient. So, around 16 earthquakes were considered in this study which had caused damages of intensity IV on MMI scale at the state capital of Tripura, Agartala. The epicentres of each of the 16 earthquakes considered for the study are shown in Fig. 26.1 as red star marks.

From the observation, it is clear that earthquakes such as the Bihar-Nepal earthquake of 1934 and the Assam earthquake of 1950 (even from further distances) damaged Agartala significantly. So, such earthquakes should be included in the assessing the seismic hazard of Tripura.

A circle of radius 700 km with its centre at Nunachara (23.805, 91.720) was chosen as the SSA to capture all the potential damaging earthquakes. The centre of the circle was considered as Nunachara since it was the centre of Tripura approximately.

Seismic Sources

Seismic sources that were not ruptured for a long period of time are more likely to rupture according to the elastic rebound theory. Considering the serious implications of the seismic gaps, this study takes into consideration of the seismic gaps as well as faults and lineaments. The faults and lineaments of India are mapped in the SEISAT [19] which was published by the Geological Survey of India (GSI). But it did not provide any information about the tectonic features and the seismic gaps around Bangladesh, Myanmar, and Tibet. Therefore, those details were taken from different studies like Yin and Harrison [46], Wang et al. [44], and Hoque and Khan [23]. ORIGIN PRO software was used for digitization of the sheets and is included in the seismotectonic map provided here. In total, 414 linear seismic sources with four seismic gaps along with the Himalayan ranges and two seismic gaps along the Sagaing fault were identified and considered for the study. The seismotectonic map prepared is presented here in Fig. 26.2.

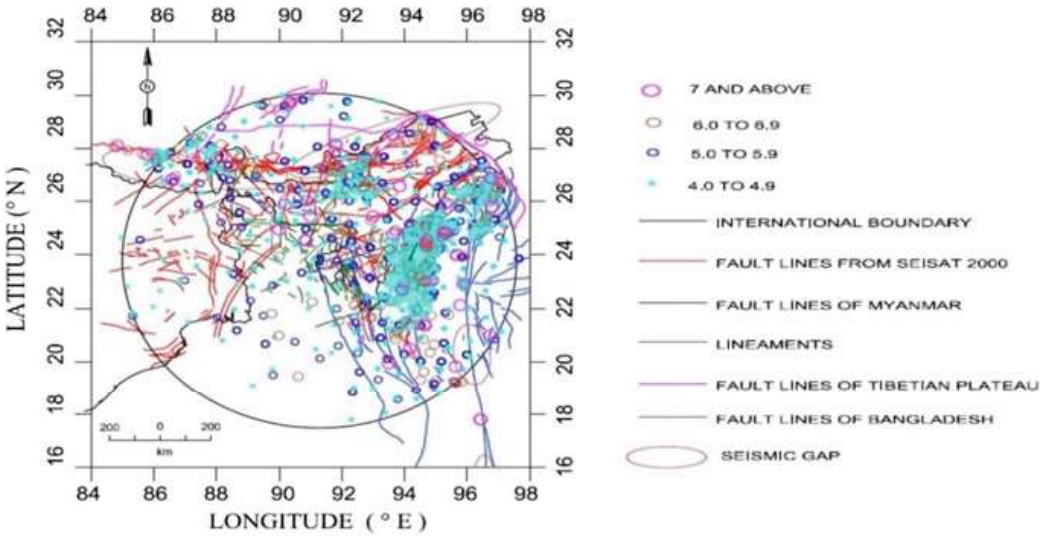

Fig. 26.2 Seismotectonic map of Tripura

Earthquake Catalogue

An earthquake catalogue was compiled for the seismic study area (SSA) in this study. So, all the earthquake events in the seismic study area (SSA) were collected from different reporting agencies like European Mediterranean Seismological Centre (EMSC), United States Geological Survey (USGS), Incorporated Research Institutions for Seismology (IRIS), and International Seismological Centre (ISC). Details of the earthquakes like date of event, time of event, depth of epicentre, magnitude, the reporting agency, magnitude scale, etc., are present in the compiled catalogue. The earthquake catalogue consisted of instrumented data of the last 121 years from 1900 to 2021.

In Fig. 26.3, a histogram of earthquake data is presented which shows the distribution of the number of earthquake events with each decade starting from 1900 to 2021.

Earthquake events compiled in this study consisted of earthquakes in different magnitude scales like M_L, M_b, M_s, and M_w. Moment magnitude (M_w) represents the energy released during any earthquake event. As M_w does not get saturated even for larger values, it is widely used for seismic hazard studies [22]. But compared to M_w, other magnitude scales like M_s, M_L, and M_s saturate at higher values and do not represent the actual released energy. So, there was a need of homogenization, i.e. converting the earthquake events that were recorded in different magnitude scales to a single magnitude scale. In this study, all the recorded events were converted to moment magnitude (M_w) using equations provided by Anbazhagan and Balakumar [5] developed for the study region (Tripura and surrounding region). There are several other conversion equations available like Sitharam and Sil [38] developed for Tripura and Mizoram, Das et al. [14] developed for the North-East India region. Beyond the magnitude ranges, Das et al. [14] was used for conversion.

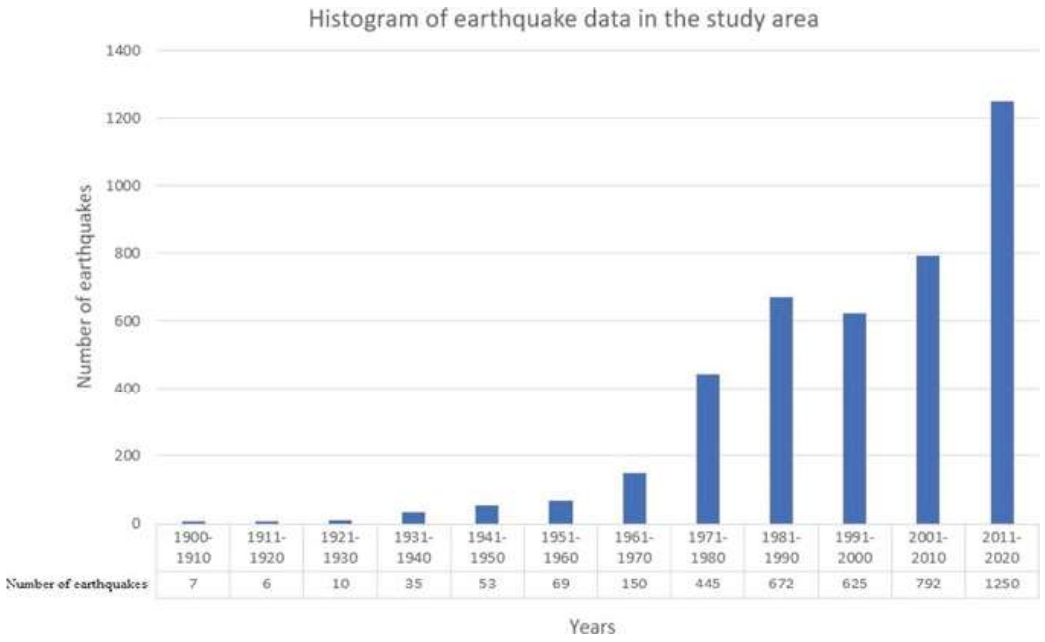

Fig. 26.3 Histogram of earthquake data

Table 26.1 Summary of the constants of the magnitude scaling equation given above

Equations	Intercept (α)	Slope (β)	R^2 value	Magnitude range
m_b to M_w	−1.5725	1.3296	0.64	4.7 to 6.6
M_L to M_w	−0.3573	1.1327	0.73	3 to 4.9
M_s to M_w	2.3172	0.6189	0.79	3 to 6.1
M_s to M_w	−0.1401	1.0238	0.68	6.1 to 6.8

The magnitude scaling equation used in this study is given below:

Anbazhagan and Balakumar [5]: General form of the equation developed for Tripura and its surrounding region: $M1 = \alpha + \beta M2$. The values of the constants in the equation are given in Table 26.1.

Uhrhammer [43], Reasenberg [34], and Gardner and Knopoff [18] are some of the widely used algorithms. In this study, Reasenberg [34] algorithm was used for declustering. The declustered catalogue contained 4114 events, which were identified as main shocks. To prepare the seismotectonic map of the SSA, superimposition of the declustered events of the catalogue was done on the fault map.

Seismicity Parameters

An earthquake catalogue is complete for a minimum magnitude, and that minimum magnitude is called magnitude of completeness. Using the Gutenberg–Richter relation given below, estimation of M_c was done.

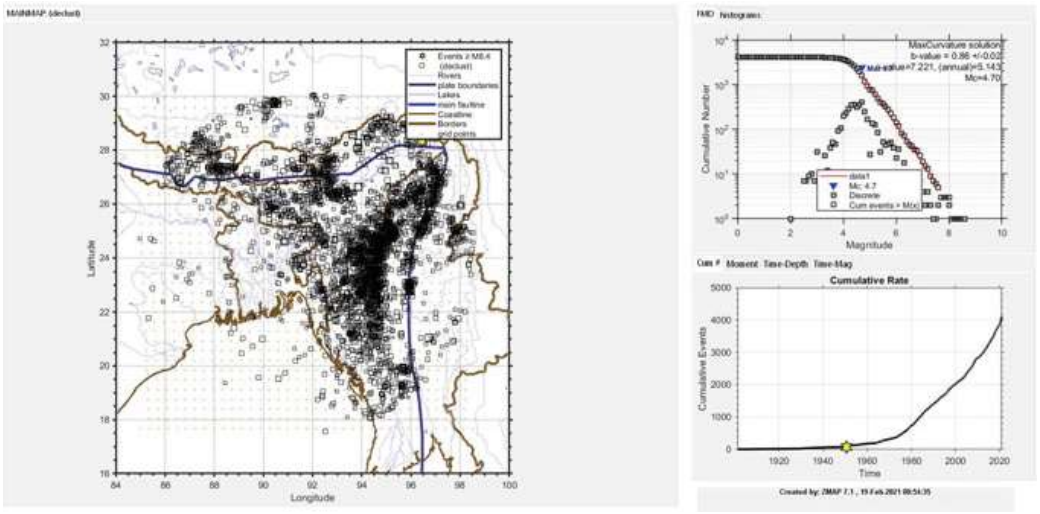

Fig. 26.4 Declustered map obtained from Zmap software

$$\log N = a + bM \tag{26.1}$$

where a is intercept, b is slope, and N is number of earthquakes of magnitude greater than M.

The magnitude of completeness (M_c) was found to be 4.7. And the seismicity parameters were found to be $a = 5.143$ and $b = 0.86$. All of these were found using Zmap software. The declustered map obtained from Zmap is presented in Fig. 26.4.

We have extrapolated the a and b value up to a magnitude of 4 due to lack of data even though the catalogue is complete for 4.7 magnitude.

Maximum Magnitude ($M_{\max}$) Estimation

$M_{\max}$ is defined as the maximum magnitude of earthquake that can be expected from a fault. Estimation of the $M_{\max}$ is a fundamental part of any hazard study. The present study makes use of three methods: the observed magnitude on each seismic source, the incremental method, and the rupture-based method which Anbazhagan et al. [4] proposed for the calculation of $M_{\max}$.

The methods used for estimating the maximum magnitude ($M_{\max}$) are described below:

Observed magnitude method: $M_{\max}$ was estimated considering the maximum observed magnitude on each fault. From the past observed seismic events record, it was found that out of 414 faults in the region, only 270 faults had an observed magnitude on it. So those 270 faults were considered in this method for hazard estimation.

Incremental method: M_{max} was estimated by adding 0.5 magnitude unit (to consider for the high seismicity of the SSA) to the maximum observed magnitude for each of the faults.

Anbazhagan et al. [4] suggested a method to estimate M_{max} of each fault by considering the regional rupture characteristics. In this method, the total length of the fault and ruptured length of the fault are considered. The subsurface rupture length (RLD) is calculated by using the widely popular relation of Wells and Coppersmith [45]. Relation given by Wells and Coppersmith is empirical which relates the subsurface rupture length (RLD) with the moment magnitude (M_W) and is given below.

$$\log(RLD) = 0.59M_W - 2.44 \tag{26.2}$$

As per Wells and Coppersmith [45], the above equation is valid for all types of earthquakes, all types of faults, and for different magnitude and distance ranges. As per Anbazhagan et al. [4], the trend between Total Fault length (TFL) and Percentage Fault Rupture (PFR) is unique and remains same for different extents of seismic study area (SSA). The plot between TFL and PFR for the radius of SSA (700 km) obtained in the present study is given below in Fig. 26.5.

In this study, the TFL was divided into three distance bins based on the trend observed and was fixed as 0–30 km, 30–160 km, and > 160 km. Corresponding to each bin, the maximum PFR was found to be 0.94, 0.70, and 0.12 respectively. Then RLD for each fault, whichever was falling in that distance bin, was increased. Now, using the same Well and Coppersmith [45] equation, the M_{max} was determined for each of the faults with their new increased RLDs. M_{max} calculated from the observed method and the incremental method was used for the conventional analysis. For the rupture-based analysis, M_{max} calculated from the regional rupture characteristics approach given by Anbazhagan et al. [4] was adopted.

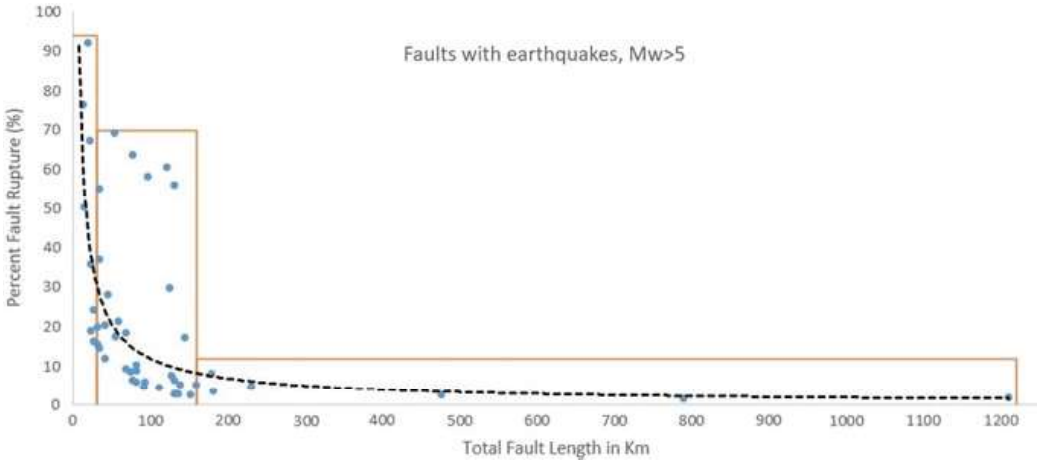

Fig. 26.5 Plot between Percentage Fault Rupture (PFR) versus Total Fault Length (TFL)

Ground Motion Prediction Equation (GMPE)

The ground motion parameters like Peak Ground Acceleration (PGA), Peak Ground Velocity (PGV), etc., at a site can be estimated using empirical equations called the Ground Motion Prediction Equations (GMPEs). Region-specific GMPEs must be selected for any site as most of the GMPEs depend on tectonic setting of the region. In this study, the SSA cannot be represented by a single GMPE as the seismic study area has a very complex tectonic framework. Therefore, based on the tectonics features and fault system, the SSA was divided into three zones.

Zone 1: Himalayan Region: Himalayan thrust zone, which is on the northern part of SSA, is demarcated by the collision of the Indian and Eurasian plates. It is believed that the tectonics in the region are due to thrusting. There is no active subduction going on in the region.

Zone 2: Indo-Burma Ranges (IBR): Indo-Burma subduction zone, which is in the eastern part of the SSA, is demarcated by the collision of Indian and Sunda plate. There are evidences that the tectonics in the region are due to subduction.

Zone 3: Bengal Basin and Shillong Plateau: This region has moderate seismicity which can be seen as the continuation of the Indo-Gangetic basin. Southern and south-western parts of the SSA are bounded by this region. No plate boundaries are present in this region.

Because of this complex setting in its tectonic features, a set of GMPEs were collected for the above-mentioned zones from the compilation of GMPEs given by Douglas [17]. The GMPEs compiled were considered to be suitable for the particular tectonic environment if they had been proposed either for the same region or similar tectonic regime worldwide.

In this study, Loglikelihood (LLH) and Data Support Index (DSI) values of each of the GMPEs are calculated using past 14 earthquakes of the region. Only the GMPEs with lowest LLH values and positive DSI values are finally selected from the set of the GMPEs.

The magnitude of the earthquake ranged between 4 and 8, and the distance ranged between 100 and 500 km. Beyond the distance and magnitude ranges, the same equations are assumed to be working. The DSI value and their weights, in parenthesis, assigned to the GMPEs for different distance ranges, i.e. 0–100 km, 100–300 km, and >300 km, have been presented in Table 26.2.

The final list of GMPEs selected based on the LLH and DSI values is summarized in the Table 26.3.

Seismic Hazard Analysis

The deterministic seismic hazard analysis (DSHA) of the study area was done using conventional methods and regional rupture-based method. In DSHA, a maximum earthquake is to be selected for each seismic source and PGA at the bedrock level for

Table 26.2 DSI values of GMPEs for different distance ranges

SL No	GMPEs	References	DSI <100 km	DSI 100–300 km	DSI >300 km
1	KT-18	Bajaj and Anbazhagan [10]	−92.6179	−36.491	−99.849
2	ANBU-13	Anbazhagan et al. [8]	−100	−100	−100
3	Kano06	Kanno et al. [26]	−100	−99.983	−100
4	ASK-14	Abrahamson et al. [1]	−97.5931	−100	−100
5	IDR-14	Idriss [24]	−96.5158	−99.872	−100
6	Zhao-06	Zhao et al. [48]	−99.125	−99.44	−100
7	SHAR-09	Sharma et al. [36]	−100	−98.93	−100
8	AMB-05	Ambraseys et al. [3]	**212.7589** ***(0.17)***	−100	−100
9	AKBO-10	Akkar and Bommer [2]	−100	−100	−100
10	ndmaH-10	NDMA [32]	−100	−100	−100
11	ndmaNE-10	NDMA [32]	−99.3728	−100	−100
12	CB-14	Campbell and Bozorgnia [12]	−10.1821	−99.886	−100
13	CY-14	Chiou and Youngs [13]	−92.4182	−96.395	−100
14	ABIF-03	Atkinson and Boore [9]	−99.8057	−98.122	−99.8057
15	ABIS-03	Atkinson and Boore [9]	−82.8113	−99.734	−82.8113
16	GT-10	Gupta [21]	−100	−99.909	−100
17	Youngs_IS97_SZ	Youngs et al. [47]	**931.6013** ***(0.55)***	**583.4183** ***(0.42)***	**801.1039** ***(1.00)***
18	Youngs_If97_SZ	Youngs et al. [47]	**422.9016** ***(0.28)***	**55.67283** ***(0.10)***	−1.25491
19	GREG-02	Gregor et al. [20]	−100	−100	−100
20	LILEIf-08	Lin and Lee [29]	−99.6573	−100	−100
21	LILEIs-08	Lin and Lee [29]	−97.1759	−99.999	−100
22	MAK-18	Mahani and Kao (2018)	−99.9882	−99.974	−100
23	SI-16	Singh et al. [37]	−99.9985	**689.645** ***(0.48)***	−100
24	NATH-12	Nath [31]	−100	−100	−100

the region due to an earthquake magnitude M_{max} on each source at the closest source to site distance is calculated. In this study, a constant average focal depth of 15 km was considered. For carrying out conventional seismic hazard analysis, the M_{max} for each source was calculated by two methods: (a) maximum observed magnitude from the past seismic events and (b) incremental method, i.e. the observed maximum magnitude for each source is incremented by adding a 0.5 moment magnitude unit to it. The incremental method was employed because of its repeated usage in the

Table 26.3 Final list of selected GMPEs

GMPE	Abbreviation of the equation	M_w range	Distance range	Standard form of equation	Coefficients value for Zero periods
Singh et al. [37]	SI-16	4 to 8.5	≤ 300	$lnln(Y_{br}) = c_1 + c_2(M_w - 6) + c_3(M_w - 6)^2 - lnR - c_4R$ where $R = \sqrt{R_e^2 + h^2}$ where Y_{br} is the Peak Ground Acceleration at bedrock level, R_e is the epicentral distance, and h is the focal depth	$c_1 = 2.0282$ $c_2 = 0.8569$ $c_3 = -0.0472$ $c_4 = 0.0091$ where c_1, c_2, c_3 and c_4 are regression coefficients
Youngs et al. [47]	Youngs-97	≥ 5	10–500	$lnln(Y) = 0.2418 + 1.414M + c_1 + c_2(10 - M)^3 + c_3 lnln\left(r_{rup} + 1.7818e^{0.554M}\right) + 0.00607H + 0.3846Z_T$ where Y is Peak Spectral Acceleration in g	$c_1 = 0$ $c_2 = 0$ $c_3 = -2.552$ $c_4 = 1.45$ $c_5 = -0.1$ where c_1, c_2, c_3, c_4 and c_5 are regression coefficients
Ambraseys et al. [3]	AMB-05	≥ 5	≤ 100	$lnln(Y) = a_1 + a_2M + (a_3 + a_4M)ln\sqrt{(d^2 + a_5^2}$ where Y is spectral acceleration in m/s^2	$a_1 = 0.835$ $a_2 = -0.083$ $a_3 = -2.489$ $a_4 = 0.206$ $a_5 = 5.60$ where a_1, a_2, a_3, a_4 and a_5 are regression coefficients

seismological community. The study area was divided into grids of $0.1^{\circ} \times 0.1^{\circ}$ (11.1 km × 11.1 km), and at the centre of each grid, PGA values were estimated.

Considering the regional rupture characteristics of all the seismic sources in the region, the rupture-based seismic hazard analysis was carried out. In this method, the M_{max} was estimated from the rupture-based method. This approach for M_{max} estimation could model the future worst-case scenario earthquake. The GMPEs were selected using the statistical procedure (based on LLH and DSI values) along with the weights. Similar grid size and interpolation technique were used to map the PGA values.

Results and Discussion

The prediction of Peak Ground Acceleration (PGA) plays a significant role in mitigating hazards caused due to earthquakes by improving the construction methods.

However, the estimated value must be realistic, and it should not be under-predicting or over-conservative. An under-predicted hazard value can cause severe damages in case of any earthquake in the region that may come in future, and if the estimated value is over-conservative, then it will be unfeasible in the sense of economy as it is same as designing any structure for such a ground motion that might ever not come in that region.

Conventional Approach

The PGA distribution map obtained from the conventional DSHA analysis has been presented in Fig. 26.6a, b. From Fig. 26.6a, it can be observed that the northern part of Tripura is more vulnerable to severe ground shaking as compared to the other parts of the state, whereas Fig. 26.6b indicates that both north and north-eastern parts of the state are vulnerable to severe ground shaking when compared to the other parts. The west and south-eastern parts of the state are liable to comparatively lesser ground shaking. The reason for this observation could be the influence of potential faults such as MBT, MCT, MFT, and Dauki fault, which are present to the north of the state.

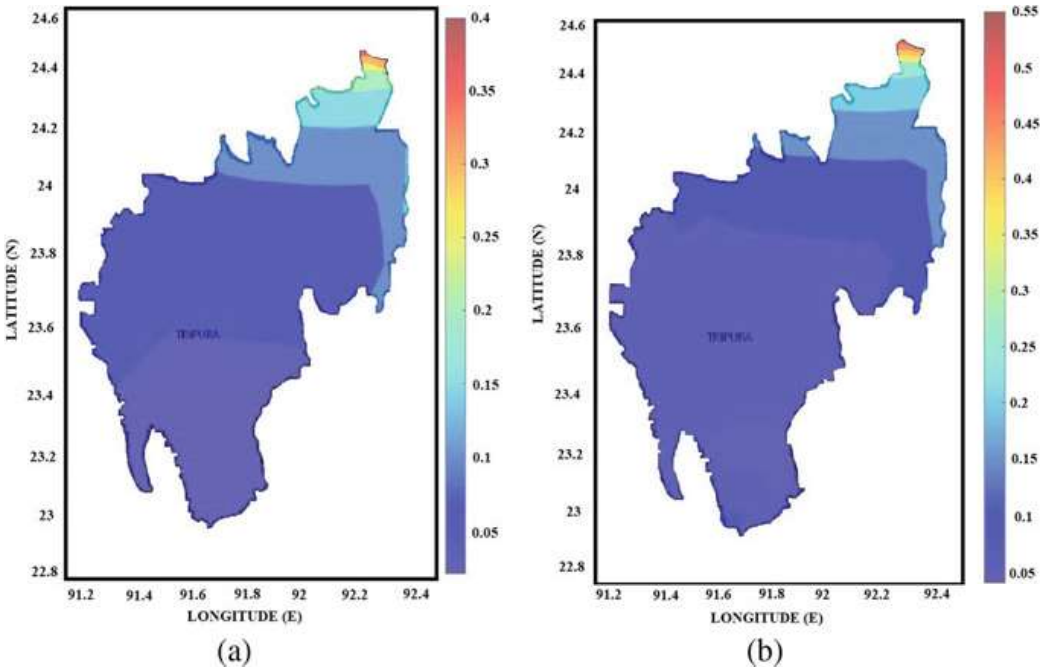

Fig. 26.6 PGA distribution map of Tripura obtained by conventional method: **a** observed magnitude approach and **b** incremental method

Rupture-Based Method

The PGA distribution map obtained from the rupture-based DSHA analysis is presented in Fig. 26.7. It can be noted from Fig. 26.7 that the north-eastern parts of the state are vulnerable to higher levels of shaking. Slightly deviating from the results of conventional analysis, the rupture-based procedure predicts a little higher levels of ground shaking for most of the southern parts of the state.

The comparison of the results of the present study with other reported literatures for this region is shown in Table 26.4. The obtained PGA values of Agartala city are matching well with the results of the study by Das et al. [15] and Sitharam and Sil [38], but do not match well with the results of the study by Sharma and Malik [34]. The reason behind this difference in results is because of the different seismic sources and GMPEs used in the studies. Das et al. [15] has used GMPE developed by them while Sharma and Malik [35] only used GMPE developed by Youngs et al. [47].

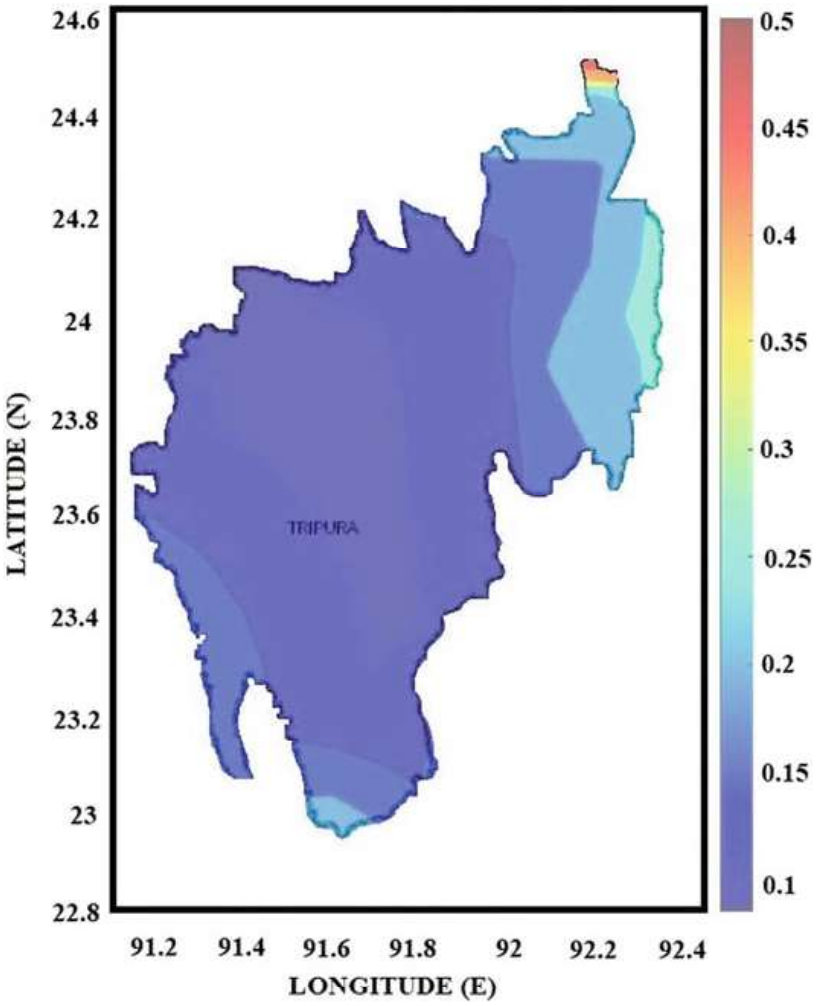

Fig. 26.7 PGA distribution map of Tripura obtained by rupture-based method

Sitharam and Sil [38] used two equations developed by Gupta [21] and Atkinson and Boore [9]. In this study, a set of GMPEs are used in combination, which were selected based on proper statistical analysis. In addition to this, the range of PGA value that the state can experience obtained by using different methods of analysis is given in Table 26.5. According to IS 1893 [25], Tripura state falls in seismic zone V which implies the highest PGA value of 0.36 g. But the present study shows that there is a spatial variation of hazard even within the small area of the state. The reason behind this variation is because at each grid points, all sources and events are considered separately.

In the present work, it was observed that the incremental method assigns larger magnitude values to such faults which have already ruptured a lot without considering their actual fault length and its potential to rupture. However, the rupture-based procedure for M_{max} calculation takes into account the rupture behaviour of the seismic sources in terms of the percentage of rupture. Since the PFR cannot take values beyond 100%, the rupture-based procedure will never produce unrealistic estimates of the maximum magnitude and thereby seismic hazard. 100% PFR would indicate the seismic source had ruptured its entire fault length. This discussion shows that the conventional technique was over-conservative in predicting hazard, whereas the rupture-based approach optimized the hazard analysis, especially when smaller active faults were considered. The rupture-based procedure could prove to be a robust tool for maximum magnitude calculation and a reliable seismic hazard study.

Table 26.4 Comparison of results with other studies

Study	PGA value (g)	Methodology of Seismic Hazard Analysis	Location	Study Area
Present study	0.10–0.22	Conventional Deterministic	Agartala	Tripura
Present study	0.14–0.20	Rupture-based Deterministic	Agartala	Tripura
Sitharam and Sil [38]	0.29	Deterministic	Agartala	Mizoram and Tripura
Sitharam and Sil [38]	0.11–0.20	Probabilistic	Agartala	Mizoram and Tripura
Das et al. [15]	0.18–0.22	Probabilistic	Agartala	North-East
Sharma and Malik [35]	0.33	Probabilistic	Agartala	North-East

Table 26.5 Summary of results obtained using different approaches

Method	Maximum observed magnitude	Incremental method	Rupture based
DSHA	0.05–0.43 g	0.05–0.57 g	0.10–0.50 g

Conclusion

Several past earthquakes, including the recent 2017 Manu earthquake of 5.7 magnitude, had shown high levels of damages, which highlight the requirement of detailed seismic hazard analysis of Tripura [7]. However, there is no region-specific seismic hazard map for the state of Tripura. In the present study, the hazard map (seismic) of Tripura was prepared by the rupture-based and conventional approach of hazard analysis. This study shows that the PGA value at bedrock level varies between 0.1 and 0.50 g for rupture-based analysis, whereas the results from conventional seismic hazard analysis show that the PGA at bedrock level varies between 0.05 and 0.57 g throughout the state. These values differ from the bedrock PGA of 0.36 g given by IS1893:2016 for the entire state. The northern part of the state is observed to be more vulnerable to hazard as compared to the rest of the state. The southern part of the state has the lowest seismic hazard potential. The capital city Agartala shows moderate hazard values. This deviation of the estimated PGA values and its spatial variation from the Indian standard code states the necessity of region-specific hazard studies. It is evident from the recent earthquake in Manu that the state of Tripura is liable to liquefaction damages as well. Therefore, it is advisable to carry out the seismic microzonation of the state to facilitate urban planning in the state. The seismic hazard analysis carried out in this study can be used for further studies such as mapping of surface ground motion, site response analysis, and liquefaction potential mapping of the state.

References

1. Abrahamson NA et al (2014) Summary of the ASK14 ground motion relation for active crustal regions. Earthq Spectra 30(3):1025–1055
2. Akkar S, Bommer JJ (2010) Empirical equations for the prediction of PGA, PGV, and spectral accelerations in Europe, the Mediterranean region, and the Middle East. Seismol Res Lett 81(2):195–206
3. Ambraseys NN et al (2005) Equations for the estimation of strong ground motions from shallow crustal earthquakes using data from Europe and the Middle East: horizontal peak ground acceleration and spectral acceleration. Bull Earthq Eng 3(1):1–53
4. Anbazhagan P et al (2015) Maximum magnitude estimation considering the regional rupture character. J Seismolog 19(3):695–719
5. Anbazhagan P, Balakumar A (2019) Seismic magnitude conversion and its effect on seismic hazard analysis. J Seismolog 23(4):623–647
6. Anbazhagan P et al (2013) Ground motion prediction equation considering combined dataset of recorded and simulated ground motions. Soil Dyn Earthq Eng 53:92–108
7. Anbazhagan P et al (2019) Reconnaissance report on geotechnical effects and structural damage caused by the 3 January 2017 Tripura earthquake, India. Nat Hazards 98(2):425–450
8. Anbazhagan P et al (2013) Estimation of design basis earthquake using region-specific Mmax, for the NPP site at Kalpakkam, Tamil Nadu, India. Nuclear Eng Des 259:41–64
9. Atkinson GM, Boore DM (2003) Empirical ground-motion relations for subduction-zone earthquakes and their application to Cascadia and other regions. Bull Seismol Soc Am 93(4):1703–1729

10. Bajaj K, Anbazhagan P (2018) Determination of GMPE functional form for an active region with limited strong motion data: application to the Himalayan region. J Seismolog 22(1):161–185
11. Bilham R (2004) Earthquakes in India and the Himalaya: tectonics, geodesy and history. Ann Geophys 47
12. Campbell KW, Bozorgnia Y (2014) NGA-West2 ground motion model for the average horizontal components of PGA, PGV, and 5% damped linear acceleration response spectra. Earthq Spectra 30(3):1087–1115
13. Chiou BS-J, Youngs RR (2014) Update of the Chiou and Youngs NGA model for the average horizontal component of peak ground motion and response spectra. Earthq Spectra 30(3):1117–1153
14. Das R, Mukhopadhyay S (2020) Regional variation of coda wave attenuation in Northeast India: an understanding of the physical state of the medium. Phys Earth Planet Inter 299:106404
15. Das S et al (2006) A probabilistic seismic hazard analysis of northeast India. Earthq Spectra 22(1):1–27
16. Debbarma J et al (2017) Preliminary observations from the 3 January 2017, MW 5.6 Manu, Tripura (India) earthquake. J Asian Earth Sci 148:173–180
17. Douglas J (2020) Ground motion prediction equations 1964–2018. http://www.gmpe.org.uk. Last accessed 2021/02/12
18. Gardner J, Knopoff L (1974) Is the sequence of earthquakes in Southern California, with aftershocks removed, Poissonian? Bull Seismol Soc Am 64(5):1363–1367
19. Dasgupta S, Narula PL, Acharyya SK, Banerjee J (2000) Geological Survey of India. Seismotectonic atlas of India and its environs, Report by Geological Survey of India
20. Gregor NJ et al (2002) Ground-motion attenuation relationships for Cascadia subduction zone megathrust earthquakes based on a stochastic finite-fault model. Bull Seismol Soc Am 92(5):1923–1932
21. Gupta I (2010) Response spectral attenuation relations for in-slab earthquakes in Indo-Burmese subduction zone. Soil Dyn Earthq Eng 30(5):368–377
22. Hanks TC, Kanamori H (1979) A moment magnitude scale. J Geophys Res: Solid Earth 84(B5):2348–2350
23. Hoque M, Khan A (2001) Seismicity and seismotectonic regionalization of the Bengal Basin, Bangladesh. Bangladesh J Geol 20:77–86
24. Idriss I (2014) An NGA-West2 empirical model for estimating the horizontal spectral values generated by shallow crustal earthquakes. Earthq Spectra 30(3):1155–1177
25. IS 1893-Part 1 (2016) Criteria for earthquake resistant design of structures—general provisions and buildings. Bureau of Indian Standards, New Delhi
26. Kanno T et al (2006) A new attenuation relation for strong ground motion in Japan based on recorded data. Bull Seismol Soc Am 96(3):879–897
27. Kayal J (2008) Microearthquake seismology and seismotectonics of South Asia, 1st edn. Springer Science & Business Media, India
28. Kundu B, Gahalaut V (2012) Earthquake occurrence processes in the Indo-Burmese wedge and Sagaing fault region. Tectonophysics 524:135–146
29. Lin P-S, Lee C-T (2008) Ground-motion attenuation relationships for subduction-zone earthquakes in northeastern Taiwan. Bull Seismol Soc Am 98(1):220–240
30. Nath S (2017) Seismic hazard, vulnerability and risk microzonation Atlas of Kolkata. Open File Report, Geoscience Division, Ministry of Earth Sciences, Government of India
31. Nath SK et al (2012) Ground-motion predictions in Shillong region, northeast India. J Seismolog 16(3):475–488
32. NDMA (2010) Development of probabilistic seismic hazard Map of India. Technical report by National Disaster Management Authority, Government of India
33. Rao GS et al (2015) A seismotectonic study of the 21 May 2014 Bay of Bengal intraplate earthquake: evidence of onshore-offshore tectonic linkage and fracture zone reactivation in the northern Bay of Bengal. Nat Hazards 78(2):895–913

34. Reasenberg P (1985) Second-order moment of central California seismicity, 1969–1982. J Geophys Res: Solid Earth 90(B7):5479–5495
35. Sharma M, Malik S (2006) Probabilistic seismic hazard analysis and estimation of spectral strong ground motion on bed rock in north east India. In: 4th international conference on earthquake engineering, Taipei, Taiwan, pp 12–13
36. Sharma ML et al (2009) Ground-motion prediction equations based on data from the Himalayan and Zagros regions. J Earthquake Eng 13(8):1191–1210
37. Singh N et al (2016) A new ground-motion prediction model for Northeastern India (NEI) Crustal Earthquakes. Bull Seismol Soc Am 106(3):1282–1297
38. Sitharam T, Sil A (2014) Comprehensive seismic hazard assessment of Tripura and Mizoram states. J Earth Syst Sci 123(4):837–857
39. Srivastava H et al (2015) Discriminatory characteristics of seismic gaps in Himalaya. Geomat Nat Haz Risk 6(3):224–242
40. Steckler MS et al (2016) Locked and loading megathrust linked to active subduction beneath the Indo-Burman Ranges. Nat Geosci 9(8):615–618
41. Stone R (2011) A Bengali recipe for disaster. Science 332(6035):1256–1258
42. Thingbaijam KKS et al (2008) Recent seismicity in northeast India and its adjoining region. J Seismolog 12(1):107–123
43. Uhrhammer R (1986) Characteristics of northern and central California seismicity. Earthq Notes 57(1):21
44. Wang Y et al (2014) Active tectonics and earthquake potential of the Myanmar region. J Geophys Res: Solid Earth 119(4):3767–3822
45. Wells DL, Coppersmith KJ (1994) New empirical relationships among magnitude, rupture length, rupture width, rupture area, and surface displacement. Bull Seismol Soc Am 84(4):974–1002
46. Yin A, Harrison TM (2000) Geologic evolution of the Himalayan-Tibetan orogen. Annu Rev Earth Planet Sci 28(1):211–280
47. Youngs R et al (1997) Strong ground motion attenuation relationships for subduction zone earthquakes. Seismol Res Lett 68(1):58–73
48. Zhao JX et al (2006) Attenuation relations of strong ground motion in Japan using site classification based on predominant period. Bull Seismol Soc Am 96(3):898–913